Radio frequency spark plug: An ignition system for modern internal combustion engines

Antonio Mariani, Fabrice Foucher

Radio frequency spark plug: An ignition system for modern internal combustion engines

Antonio Mariani *, Fabrice Foucher

Univ. Orléans, 8 rue Léonard de Vinci, Orléans 45072, France

Plasma sustained ignition systems are promising alternatives to conventional spark plugs for those applications where the conditions inside the combustion chamber are more severe for spark plug operation, like internal combustion engines with high compression ratio values or intake charge dilution.

This paper shows the results of an experimental activity performed on a spark ignition internal combustion engine equipped with a Radio Frequency sustained Plasma Ignition System (RFSI). Results showed that the RFSI improved engine efficiency, extended the lean limit of combustion and reduced the cycle-by-cycle variability, compared with the conventional spark plug for all test conditions. The adoption of the RFSI also had a positive impact on carbon monoxide and unburned hydrocarbon emissions, whereas nitrogen oxide emissions increased due to higher temperatures in the combustion chamber. Therefore, RFSI represents an innovative ignition device for modern internal combustion engines and overcomes the compatibility problems of other non-conventional ignition systems.

1. Introduction

Ignition systems in internal combustion engines are fundamental for engine efficiency and pollutant emissions. Conventional spark ignition systems store the electrical energy in a magnetic coil and discharge it through the electrode gap of the spark plug, located in the combustion chamber. It is necessary to have a proper air–fuel mixture composition around the spark plug gap at the ignition timing in order to generate a flame kernel that can propagate through the combustion chamber. The energy transfer to the in-cylinder air–fuel mixture is not optimal as just a small amount of the electrical energy is absorbed.

Although the adoption of high compression ratio values, charge dilution and lean air–fuel mixtures in spark ignition engines improves engine efficiency and exhaust emissions [1–3], it limits the use of conventional spark plugs. In fact, lean air–fuel mixture reduces the probability of having a flammable composition at the ignition timing between the spark plug electrodes; the dilution reduces the combustion speed and highly diluted mixtures are difficult to ignite [4–6]; higher compression ratios cause higher in-cylinder pressure values at the end of the compression stroke, with an impact on the breakdown characteristics [7–9]. Consequently, the spark plug operates under more severe combustion chamber conditions and the adoption of conventional ignition systems can result in incomplete combustion or misfires.

Efforts have been focused on the improvement of conventional ignition systems or on the development of alternative methods for initiating combustion.

High energy ignition systems are usually extensions of the basic ignition systems [10]. Enhanced designs attempt to increase and improve the delivery of ignition energy to the air–fuel mixture.

* Corresponding author. Tel.: +33 (0) 2 38 49 24 57; fax: +33 (0) 2 38 41 73 83.
E-mail address: antonio.mariani@univ-orleans.fr (A. Mariani).

Nomenclature

CO	carbon monoxide
CO_2	carbon dioxide
COV	coefficient of variation
deg	degree
EGR	exhaust gas recirculation
HFIS	high frequency ignition system
HC	hydrocarbon
imep	indicated mean effective pressure
isfc	indicated specific fuel consumption
N_2	nitrogen
NO*x*	nitrogen oxides
RFSI	Radio Frequency Ignition System
RLC	resistance inductance capacitance
rpm	rotations per minute
TDC	top dead center
ϕ	equivalence ratio

The spark plug electrode geometry can be designed in order to reduce heat loss from the flame kernel and speed up the kernel growth [11]. The electrode material is also important to improve service life, ignitability, pre-ignition protection and fouling resistance [12]. Multiple spark plugs in one cylinder have also been used. The advantages are a reduced flame travel distance, increased tolerance to EGR, possible use of higher compression ratios with a given fuel and improvements in fuel efficiency [13]. Other solutions have been explored, like increasing the number of electrodes on the plug [14] or the adoption of pre-combustion swirl chambers [15]. Though these methods shows some improvement in the effectiveness of delivering energy to the air–fuel mixture, they are still subjected to the problems of conventional spark plugs, like electrode erosion, fouling and small spark volume. Laser ignition has also been the subject of a number of research efforts but it is still far from being a practical solution for internal combustion engines [16]. Laser-induced spark ignition of methane–air mixtures has been investigated in [17], demonstrating that the system fails to ignite methane–air mixtures close to the lower flammability limit.

The plasma sustained ignition systems are a promising alternative to conventional spark plugs. Several solutions have been proposed for plasma generation. Plasma jet igniters and rail plug igniters use electrical discharges inside small volume cavities. The ionized spark kernel is immediately moved away from the housing where it is created, to a location within the combustion chamber where the thermodynamic conditions are more favorable for rapid flame growth. Experiments performed applying plasma jet igniters to production and research engines [18–22] show the extensions of lean operation and the improvements in engine efficiency at all engine loads. Exhaust emission measurements show no differences for CO and HC emissions, while NO*x* levels are higher with the plasma jet systems due to faster combustion. The high electrical current discharge in this device tends to cause high erosion of the electrodes. The rail plug gives similar results and does not overcome the metal erosion problems [23,24].

[25] describes the results obtained with a high frequency ignition system (HFIS) which generates high voltage using the principle of the resonator in a RLC circuit. The HFIS has been compared with a Delphi multi-spark ignition system. Both ignition systems have been tested on a single cylinder engine at various engine loads, speeds and exhaust gas recirculation rates, with both homogenous and stratified air–fuel mixtures. Results show comparable combustion characteristics during the homogenous combustion mode whereas, during the stratified operation, the combustion is more stable and the tolerance to EGR increases with the HFSI.

Microwaves have been adopted to enhance the plasma generated by a spark plug [26–28]. The microwaves are transmitted using different configurations for the antenna. Test demonstrated that the ignition limits extend and the combustion stability increases at diluted conditions using the microwave-assisted spark plug compared to the spark-only mode. In [29] microwaves have been used to enhance the plasma generated with a capacitive discharge spark. The tests, performed in a constant volume combustion chamber for various methane–air mixtures, demonstrated that the flame kernel growth rate and size increase using the microwave-assisted spark plug compared to the spark-only mode, whereas the flame rise time does not change, indicating that the microwave system only affects early heat release rates and flame kernel growth.

Other studies investigated the corona generated plasma [30,31], where the energy is transferred to the gases through the electric field, carried out by electrons and stored in molecules as internal energy. High-energy electrons collide with the molecules of fuel and oxygen, generating highly reactive radicals that promote oxidation chain reactions. The discharge takes a multi-channel pattern and heats up if sustained with high voltage, reaching ignition temperatures. The mechanisms of non-equilibrium plasma for ignition and combustion have been examined in depth in [32,33]. In [34] high-speed pulsed plasma is generated in a coaxial electrode system producing a volumetric discharge. Authors found that, adopting the high-speed pulsed plasma ignition system, the flame development angle reduces and the mixture ignitability improves, in particular under lean combustion conditions, compared with the conventional spark plug.

This paper shows the results of an experimental activity performed on a spark ignition engine equipped alternatively with a conventional spark plug and a Radio Frequency Ignition System (RFSI) developed by Renault [35]. The RFSI sustains and heats up a multi-channel discharge [36–38]. The application of an alternative radio frequency voltage keeps the electrons close to the spark plug electrode, impeding the formation of the electric arc. A resonant RLC circuit is required, including an inductance inside the spark plug. The RFSI ignites a volume bigger than standard spark plugs due to the absence of the ground electrode, has a higher efficiency of the ignition energy delivery and ability to vary the spark duration depending on engine operating conditions. The RFSI has been designed to assure integration in actual internal combustion engines, in terms of compatibility and energy consumption. Results show that the adoption of the RFSI improves engine efficiency at all test conditions, extends the lean limit of combustion and reduces CO and HC emissions compared with the standard spark plug.

2. Experimental setup

The test engine, whose main characteristics are reported in Table 1, was modified in the admission and exhaust manifolds for allowing single cylinder operation. It was coupled with a permanent magnet servomotor manufactured by Parvex.

An Environment S.A. multi-range gas analyzer was employed to measure carbon monoxide (CO), carbon dioxide (CO_2), unburnt hydrocarbons (HC), nitrogen oxides (NO*x*) and oxygen (O_2). A

Table 1
Engine characteristics.

Engine type	L4 turbocharged spark ignition
Injection type	Direct injection
Displacement	1598 cm^3
Bore × stroke	77 mm × 85.8 mm
Compression ratio	10.5
Rated power	110 kW at 5800 rpm
Torque	240 Nm at 1400 rpm

non-dispersive infrared analyzer was used for CO and CO_2, a paramagnetic detector for O_2, a flame ionization detector analyzer for HC, and a chemiluminescence analyzer for NO*x*. Their accuracy is in the range ±1% of reading. The carbon balance method was used for the fuel consumption determination.

In-cylinder pressure was measured by means of an AVL water cooled piezoelectric pressure sensor. Its measuring range is 0-250 bar with a sensitivity of 19 pC/bar. In-cylinder pressure data were acquired over 100 consecutive engine cycles with a resolution of 0.1 crank angle (CA) degree at all operating conditions. The overall uncertainty on the pressure measurement is below 2% of the measured value. A Kistler crankshaft encoder provided crank position data and was dynamically aligned with engine TDC using an AVL TDC probe.

A heat release analysis was performed on the basis of the in-cylinder pressure data. The algorithm developed for data processing is based on a single zone model which determines the heat release using the first law of thermodynamics. The model assumes that the pressure is homogeneous inside the combustion chamber, the specific heat a function of the temperature only. The in-cylinder mass takes into account the intake air, the internal exhaust gas recirculation and mass of fuel. The chemical species considered are: CO_2, H_2O, O_2, CO, H_2 and N_2. The heat transfer through the cylinder walls is calculated with the Woschni model [39]. The equivalence ratio is determined using the "five gas exhaust analysis" [40] and depends on exhaust composition. The uncertainty on the heat release rate determination is largely dominated by the accuracy of the pressure transducer and the angle encoder.

The test conditions were 1400 rpm with engine loads of 4 bar, 6 bar, 8 bar and 10 bar of indicated mean effective pressure (imep).

Table 2
Experimental conditions.

Imep (bar)	4, 6, 8, 10
Engine speed (rpm)	1400
Dilution with N_2 (%)	0, 10, 20, 30
Equivalence ratio	$0.6 \leqslant \phi \leqslant 1$

The spark timing was adjusted to maximize the imep (max imep spark advance), [41]. The equivalence ratio was reduced from $\phi = 1$ untill the condition where the coefficient of variation of imep was 5%. Intake air was also diluted with 10%, 20% and 30% nitrogen. Dilution of the intake charge is usually realized by means of exhaust gas recirculation. In order to estimate the difference between EGR and nitrogen dilution in terms of impact on the in-cylinder gas temperature, the heat capacity of the diluents is calculated and plotted versus the equivalence ratio, Fig. 1(a), and versus the dilution rate, Fig. 1(b).

The intake gas composition and properties in the case of dilution with EGR are determined according to Eq. (1), where τ is the EGR rate and e the excess of air:

$$\begin{aligned} &C_xH_y + (1-\tau)(1+e)(x+\tfrac{y}{4})(O_2+3.78N_2)+ \\ &+\tau\left[\tfrac{1}{1-\tau}(xCO_2+\tfrac{y}{2}H_2O+3.78(x+\tfrac{y}{4})N_2)+(1+e-\tfrac{1}{1-\tau})(x+\tfrac{y}{4})(O_2+3.78N_2)\right] \\ &\rightarrow \tfrac{1}{1-\tau}(xCO_2+\tfrac{y}{2}H_2O+3.78(x+\tfrac{y}{4})N_2)+(1+e-\tfrac{1}{1-\tau})(x+\tfrac{y}{4})(O_2+3.78N_2) \end{aligned} \quad (1)$$

Test operating conditions are summarized in Table 2. The engine was equipped alternatively with the RFSI and the standard spark plug and fuelled with isooctane.

3. Spark plugs

In a standard spark plug, the ignition takes place between the central electrode and the ground electrode, Fig. 2(a), and receives the high voltage from the secondary circuit of a conventional ignition coil.

In the RFSI an alternating, high voltage, electrostatic field generates excitation of high-energetic electronic states and ionization, increasing the number of free radicals. These radicals are

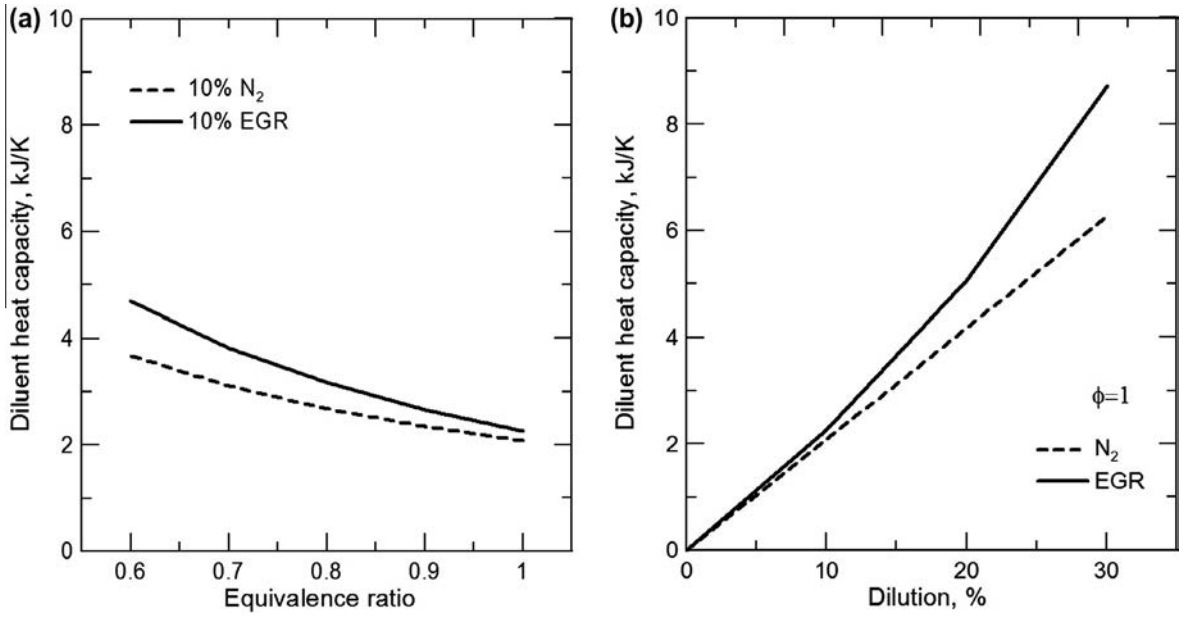

Fig. 1. Variation of diluents heat capacity in case of dilution with exhaust gas recirculation and nitrogen.

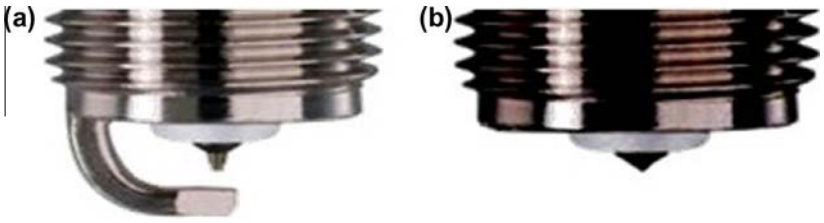

Fig. 2. Standard (a) and radio frequency (b) spark plugs.

responsible for chemical reactions in the air–fuel mixture which proceed exothermically, activating the combustion process. A relatively large amount of ionizing energy, up to an order of magnitude greater than conventional ignition systems, can be delivered to the combustion chamber. The electrostatic low intensity current characteristic of the spark does not require the second electrode.

The RFSI is composed of a resonant transformer circuit, Fig. 3, which amplifies the input voltage delivered by an external supply unit. At the resonance frequency, which is 4.97 MHz for the tested spark plug, the voltage amplitude reaches its maximum. Depending on the in-cylinder thermodynamic conditions, the breakdown voltage can be reached and the ignition initiated. The supply of the input voltage is driven by a function generator which allows the control of the RFSI operating parameters which are reported in Table 3. The electrode voltage increases during the initial transient, Fig. 4(a), as the excitation signal is supplied at the resonant frequency of the RLC circuit. If the breakdown conditions are attained, the discharge is formed and the electrode voltage drops as in Fig. 4(b). The spark takes a multi-channel structure, with filament lengths proportional to the applied voltage and in-cylinder gas density, allowing the ignition of a volume bigger than that of a standard spark plug. The electrode voltage envelope changes if one of the filaments reaches a metallic ground. In this case, the arc is formed and the voltage falls instantaneously to zero. This operating condition should be identified rapidly and avoided.

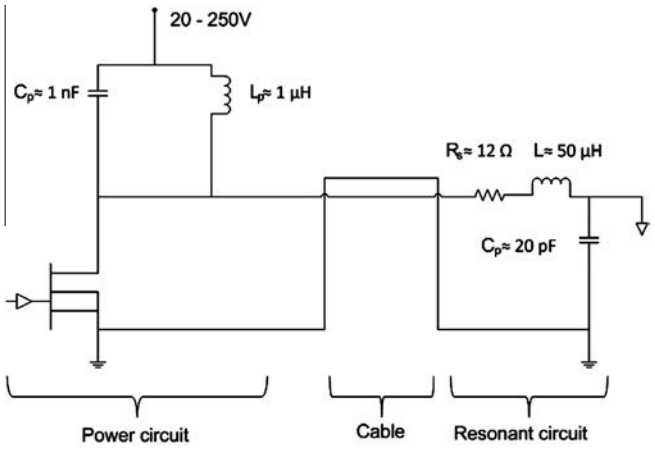

Fig. 3. RFSI electric circuit.

Table 3
RFSI operating parameters.

Ignition events per engine cycle	1
Spark duration	500 µs
Frequency	4.967 MHz
Input voltage	100–150 V

The energy transferred to the in-cylinder gases can be determined with Eq. (2) where U is the input voltage, I the current flowing through the spark plug and R its equivalent resistance.

$$E_{spark} = \int_0^t UI\,dt - R\int_0^t I^2\,dt \tag{2}$$

The resistance R can be determined when $E_{spark} = 0$ under misfire conditions, where the ignition energy is completely dissipated by the Joule effect, Eq. (3).

$$R = \frac{\int_0^t UI\,dt}{\int_0^t I^2\,dt} \tag{3}$$

Measurements performed on the RFSI returned a value of the equivalent resistance of 14.7 Ω. A detailed description of the RFSI and the analysis of the RFSI's ignition energy are available in [35,38].

4. RFSI electrode configuration

Tests were initially performed with two electrode configurations for the RFSI: the single electrode (RFSI A) and the five electrodes (RFSI B), Fig. 5. The results obtained with the engine equipped alternatively with the RFSI A and B are reported in this section.

The flame development angle (the interval between the spark discharge and 10% mass fraction burned crank angle) is plotted in Fig. 6 versus the equivalence ratio, for the two RFSI electrode configurations, without dilution (solid lines) and with 20% intake air dilution with nitrogen (dashed lines), in order to evaluate the effect of the electrode geometry on the early stages of the combustion process. Without dilution, the RFSI B promotes faster flame development than the RFSI A at equivalence ratio values between 1 and 0.7. At equivalence ratio values lower than 0.6, the flame development is faster with the RFSI A. With 20% nitrogen dilution, the flame development angle is smaller with the RFSI A compared with the RFSI B at equivalence ratio values lower than 0.9. The RFSI A also shows a more stable combustion than the RFSI B as shown in Fig. 7 where the coefficient of variation of imep (COV_{imep}) [40] is plotted versus the equivalence ratio. In fact, at low equivalence ratio values and with 20% nitrogen dilution, the cyclic variability is lower with the RFSI A than for RFSI B.

The comparison performed in this section allows understanding the effect of the electrode configuration on the development of the combustion process. Increasing the number of the electrodes of the RFSI causes an increase of heat losses. As a consequence, the engine is less stable with the RFSI B compared to the RFSI A at low equivalence ratio values and with dilution, where the energy required for igniting the mixture increases and the energy transfer process becomes more important.

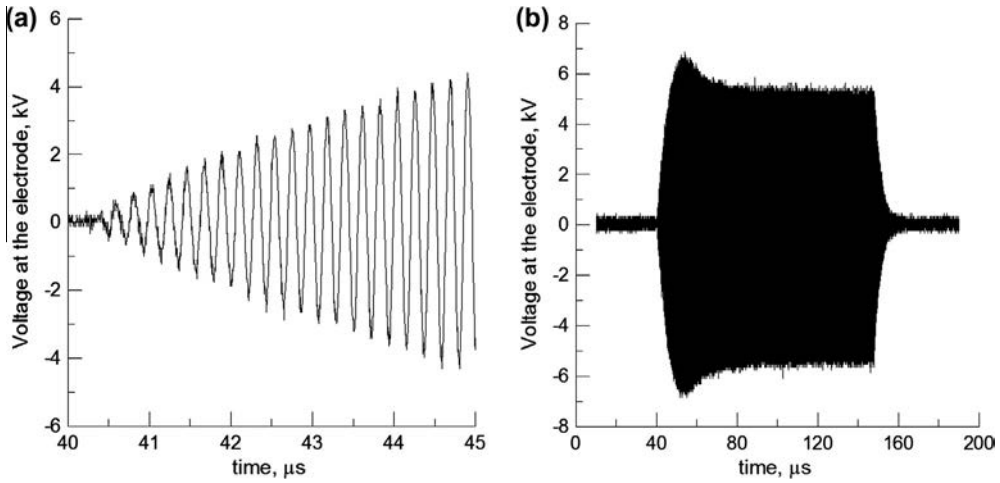

Fig. 4. RFSI's electrode voltage versus time at 6 bar imep and $\phi = 0.6$. RFSI input voltage 100 V; Excitation signal frequency 4.967 MHz.

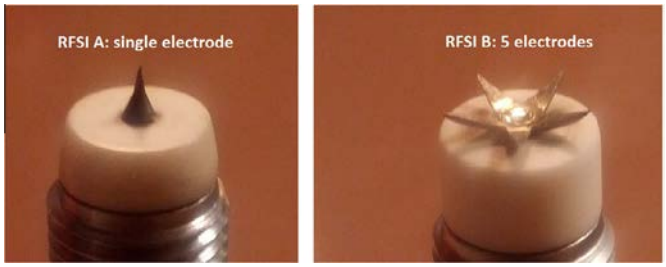

Fig. 5. Radio frequency ignition system with one electrode and 5 electrodes.

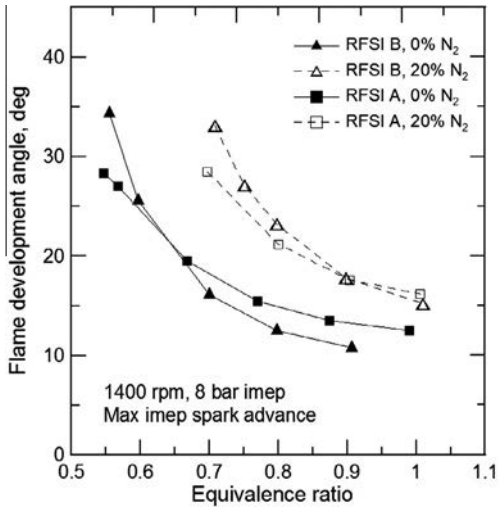

Fig. 6. Flame development angle (0–10% burned) versus the equivalence ratio, at 0% and 20% intake air dilution with nitrogen, with the RFSI A and RFSI B.

5. RFSI and standard spark plug

This section compares the results obtained with the RFSI A and the standard spark plug.

5.1. Combustion analysis

The analysis of in-cylinder pressure data characterized the effects of the ignition system on the combustion process.

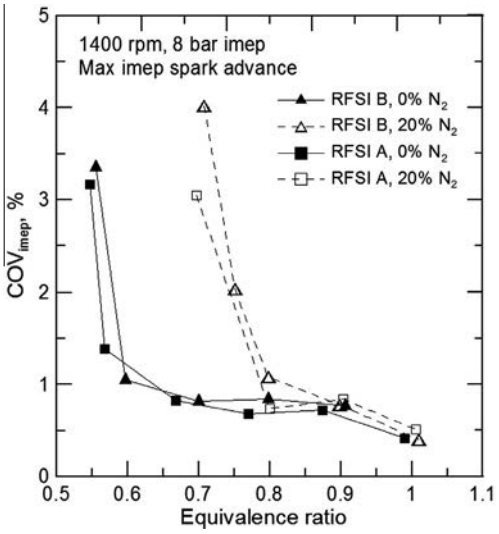

Fig. 7. Coefficient of variation of indicated mean effective pressure versus the equivalence ratio, at 0% and 20% intake air dilution with nitrogen, with the RFSI A and RFSI B.

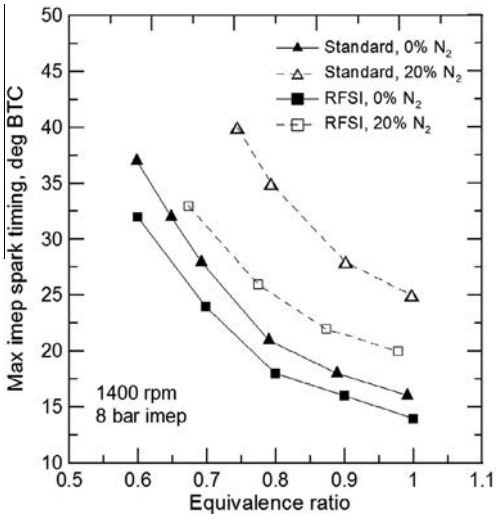

Fig. 8. Spark timing for maximum imep versus the equivalence ratio, with 0% and 20% intake air dilution with nitrogen.

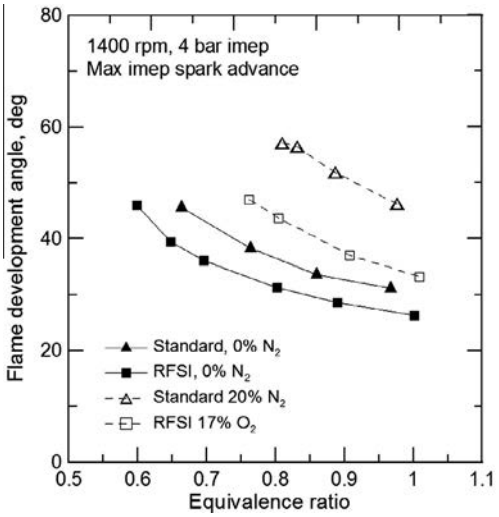

Fig. 9. Flame development angle (0–10% burned) versus the equivalence ratio, with 0% and 20% intake air dilution with nitrogen.

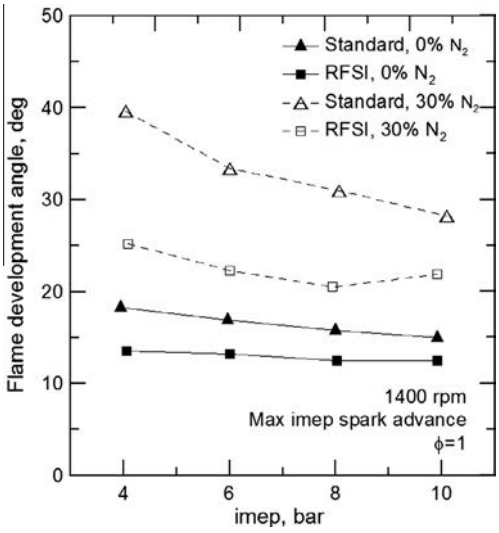

Fig. 10. Flame development angle (0–10% burned) versus imep, at 0% and 30% intake air dilution with nitrogen.

Fig. 8 shows the spark timing for the maximum imep versus the equivalence ratio, without dilution (solid lines) and with 20% intake air dilution with nitrogen (dashed lines), for both the RFSI and the standard spark plug. The advance required for the max imep increases as the equivalence ratio is reduced. The max imep spark timing with RFSI is always delayed compared with the standard spark plug due to the impact of the radio frequency ignition system on the combustion speed.

Fig. 9 shows the effects of the ignition system on the flame development angle, here defined as the angle between the ignition and 10% of heat release. RFSI promotes a more rapid initial flame growth compared to the standard spark plug, with a reduction of the flame development angle at all operating conditions. The flame development is enhanced with use of the RFSI as more energy can be transferred to the plasma, generating highly reactive radicals which promote oxidation chain reactions. With the standard spark plug, under thermal ignition conditions, the ignition delay depends upon the rate of the dissociation reactions, which are endothermic, and the induction delay time is greatly affected by temperature. Furthermore, the multi-channel structure of the RFSI discharge ignites a volume bigger than a standard spark plug which is limited by the inter-electrode distance. The dilution with nitrogen increases the heat capacity of the air–fuel mixture and decreases the heat release rate causing a reduction of the combustion speed [40]. As a consequence, the flame development angle increases, with variations between 45% and 65% compared to the case without dilution, when the engine is equipped with the conventional spark plug. With the RFSI the effect of dilution on combustion speed is attenuated, with an increase of the flame development angle ranging between 30% and 46% compared to tests without dilution.

Fig. 10 shows the effect of the engine load variation on the flame development angle at $\phi = 1$ with 0% and 30% intake air dilution with nitrogen. As imep is reduced, the residual burned gas fraction increases, and the flame development angle as well. This trend is more evident when the standard spark plug is used, in particular with 30% nitrogen dilution.

The impact of the RFSI on the combustion speed is also shown in Fig. 11, where the heat release rate is plotted versus the crank angle. The maximum value of heat release rate increases, the combustion duration reduces and the angular position of the maximum heat release rate advances with the RFSI compared to the standard spark plug. The increment of heat release rate peak caused by the RFSI is about 8% compared with the standard spark plug at

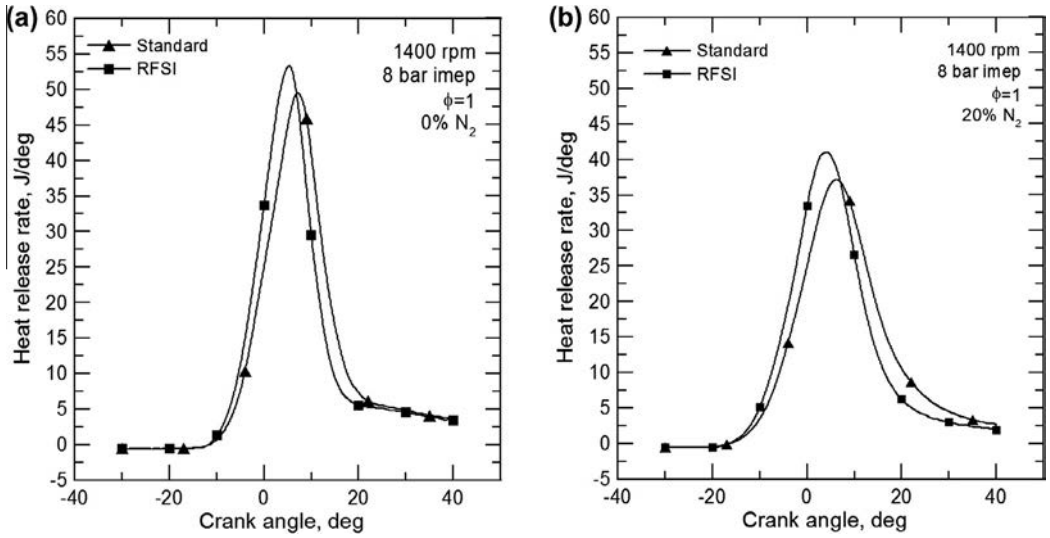

Fig. 11. Heat release rate versus crank angle.

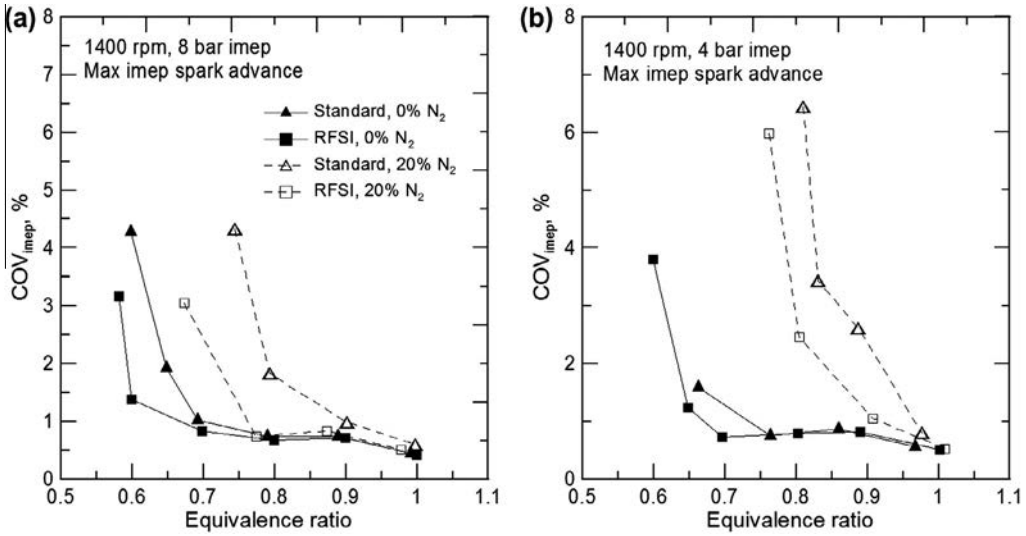

Fig. 12. Coefficient of variation of indicated mean effective pressure versus the equivalence ratio, with 0% and 20% intake air dilution with nitrogen.

stoichiometric conditions without dilution, Fig. 11(a). The effect is more evident with dilution, as shown in Fig. 11(b), with an increment of the heat release rate peak of 10% when the RFSI is used. In fact, as dilution reduces the burning speed, the impact of a fast flame development promoted by the RFSI becomes more important.

The coefficient of variation of indicated mean effective pressure, COV_{imep}, is reported in Fig. 12 versus the equivalence ratio. At 8 bar imep, Fig. 12(a), without dilution, the COV_{imep} is reduced with the RFSI compared with the standard spark plug for equivalence ratio values lower than 0.8. With 20% nitrogen dilution, the positive effect of the RFSI on combustion stability is important for equivalence ratio values lower than 0.9. The improvement of combustion stability caused by the plasma ignition is also evident at lower engine loads, as shown in Fig. 12(b).

Fig. 13 shows the effect of the engine load on the combustion stability at $\phi = 1$, without dilution and with 30% nitrogen dilution. Without dilution the COV_{imep} values are low with both ignition systems at all engine loads. With 30% nitrogen dilution, the combustion stability reduces at low engine loads when the standard spark plug is used whereas the RFSI promotes better stability as it limits the appearance of slow burning engine cycles. Fig. 14 shows the COV_{imep} versus the dilution rate with nitrogen, at $\phi = 1$ and $\phi = 0.9$. At stoichiometric conditions, the stability is good with both ignition systems at all dilution rates. At $\phi = 0.9$, the COV_{imep} sharply increases with the standard spark plug at 30% dilution, attaining a value of 3.5% whereas good combustion stability is observed at all dilution rates when the RFSI is adopted. Results demonstrate that the plasma ignition promotes a stable combustion under highly diluted conditions.

5.2. CO_2 emissions and fuel consumption

This section describes the indicated specific CO_2 emissions and fuel consumption.

Fig. 15 shows indicated specific CO_2 emissions versus the equivalence ratio ϕ at 8 bar (a) and 4 bar (b) of indicated mean effective pressure (imep), without dilution (solid lines) and with 20% intake air dilution with nitrogen (dashed lines). At 8 bar imep, $\phi = 1$, without dilution, CO_2 emissions are 679 g/kW h and 664 g/kW h with

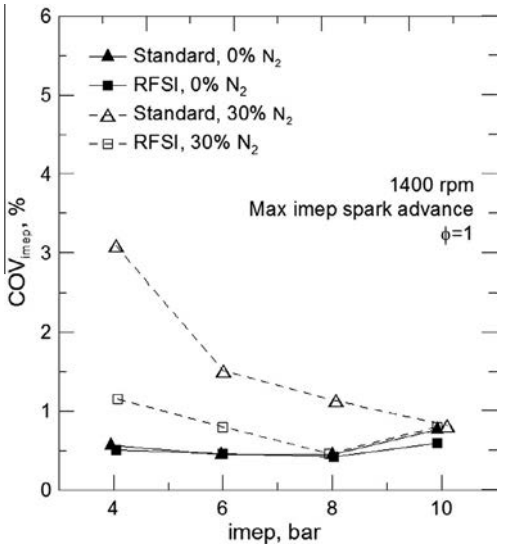

Fig. 13. Coefficient of variation of indicated mean effective pressure versus imep, at 0% and 30% intake air dilution with nitrogen.

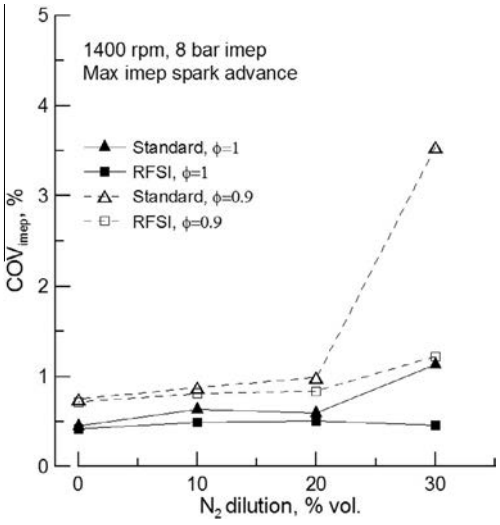

Fig. 14. Coefficient of variation of indicated mean effective pressure versus the dilution rate with nitrogen at equivalence ratios $\phi = 1$ and $\phi = 0.9$.

the standard spark plug and the Radio Frequency Spark Plug (RFSI) respectively. At lower equivalence ratio values, the gap between the ignition systems increases, as at $\phi = 0.6$, where CO_2 emissions are 630 g/kW h and 596 g/kW h with the standard spark plug and RFSI respectively. The dilution with nitrogen reduces fuel consumption and, as a consequence, CO_2 emissions. At lower engine loads, Fig. 15(b), carbon dioxide emissions increase due to the increase of fuel consumption.

The indicated specific fuel consumption (isfc) is plotted in Fig. 16 versus the equivalence ratio for the two spark plugs, for 0% and 20% intake air dilution with nitrogen, to evaluate the impact of the ignition systems on the engine efficiency. At 8 bar imep, Fig. 16(a), the isfc is 233 g/kW h with the standard spark plug and 228 g/kW h with RFSI at $\phi = 1$ without dilution, with an increase of the engine efficiency of 2.3%. The minimum isfc with the RFSI is at $\phi \approx 0.6$, with 5% reduction of the fuel consumption compared with the standard spark plug. The minimum isfc is 210 g/kW h at $\phi \approx 0.65$ with the standard spark plug and 200 g/kWh at $\varphi \approx 0.6$ with the RFSI. With 20% nitrogen dilution, the engine efficiency increases due to lower in-cylinder temperature, reduced burned gases dissociation and decreased heat losses to the walls of the combustion chamber. In this case, the stability limit is at $\varphi \approx 0.75$ with the standard spark plug and at $\phi \approx 0.65$ with the RFSI. The reduction of the engine load at constant speed causes an increase of the isfc, Fig. 16(b), due to the increased pumping work and the increased importance of heat transfer.

The difference between the trends of carbon dioxide emissions and fuel consumption at very low equivalence ratio values is the consequence of a reduction of the combustion efficiency. In fact, at very low equivalence ratio values, slow burning cycles become more frequent and cycle-by-cycle variation increases, causing an increase of CO and HC emissions.

The RFSI shows lower isfc than the standard spark plug due to higher engine efficiency promoted by the faster combustion.

5.3. Exhaust emissions

This section summarizes the results obtained with the two ignition systems in terms of indicated specific CO, HC and NO*x* emissions.

CO emissions are plotted in Fig. 17 versus the equivalence ratio. At 8 bar imep, Fig. 17(a), the RFSI provides a substantial benefit to CO emissions, particularly near $\phi = 0.6$. With dilution, the positive effect of the RFSI is important over the whole range of equivalence

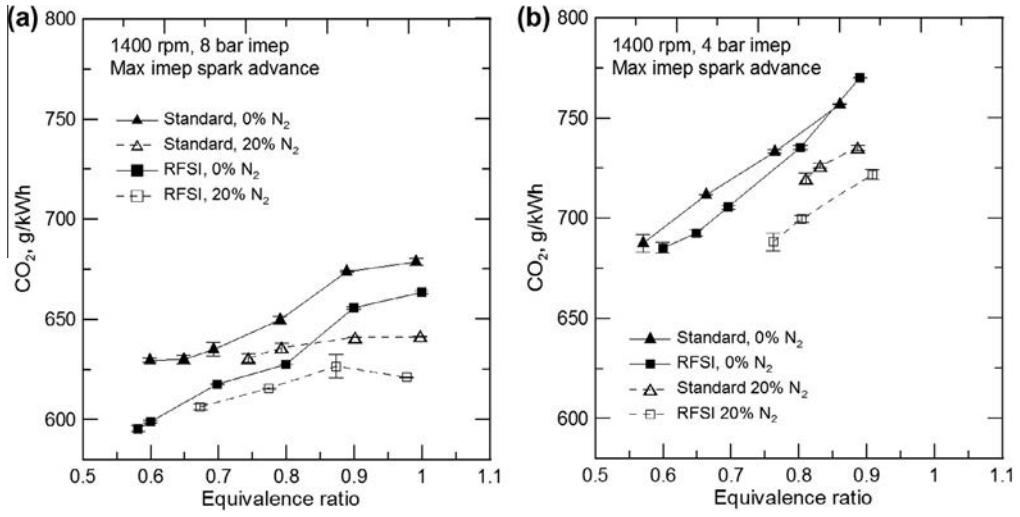

Fig. 15. Indicated specific CO_2 emissions versus the equivalence ratio, with 0% and 20% intake air dilution with nitrogen.

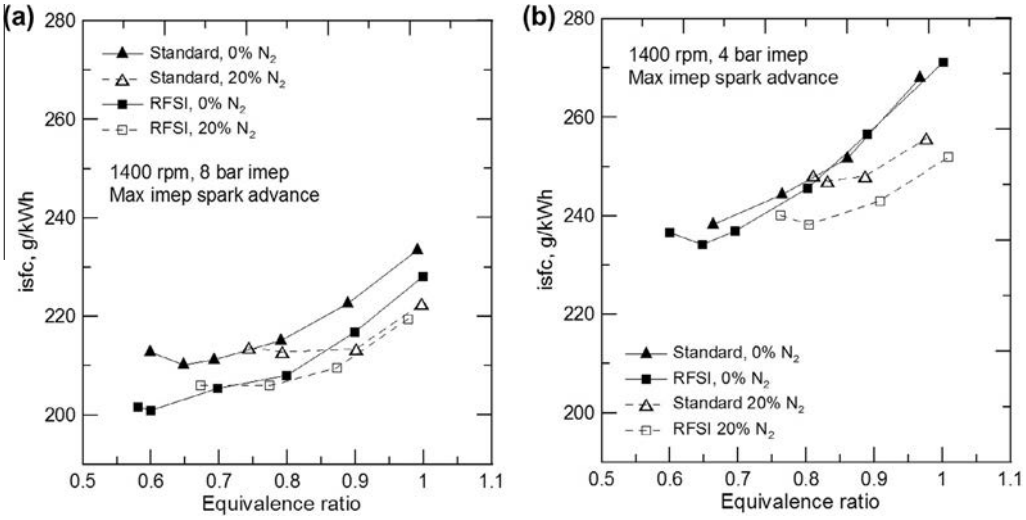

Fig. 16. Indicated specific fuel consumption versus the equivalence ratio, with 0% and 20% intake air dilution with nitrogen.

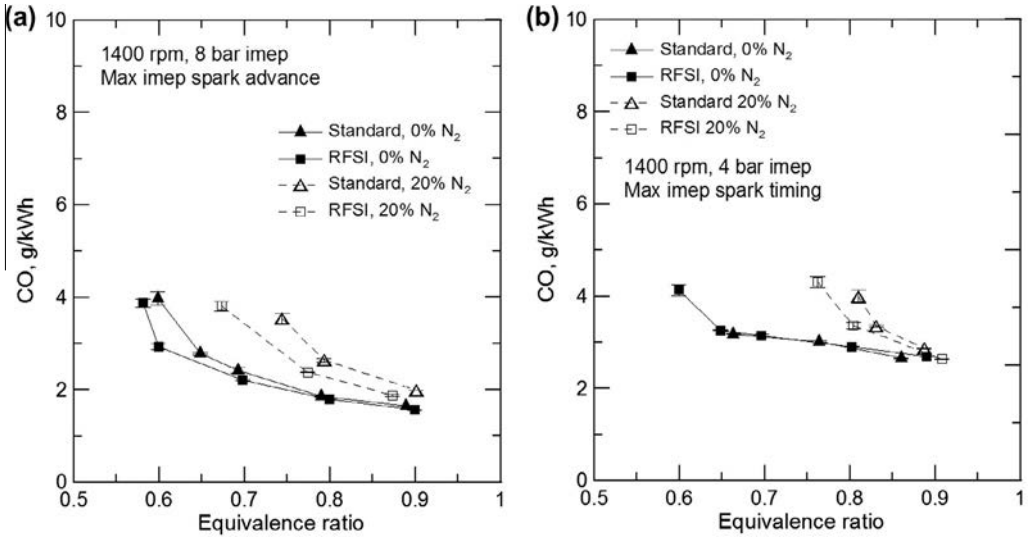

Fig. 17. Indicated specific CO emissions versus the equivalence ratio, with 0% and 20% intake air dilution with nitrogen.

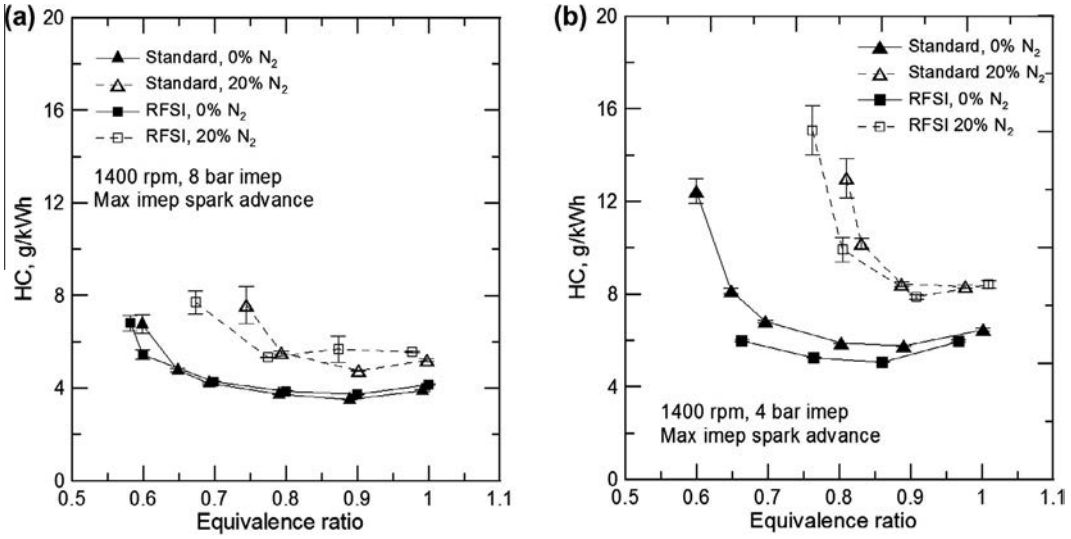

Fig. 18. Indicated specific HC emissions versus the equivalence ratio, with 0% and 20% intake air dilution with nitrogen.

ratio values. Similar results have been observed at different engine loads, as described in Fig. 17(b) at 4 bar imep.

Fig. 18 shows the HC emissions obtained with the two ignition systems. At 8 bar imep, Fig. 18(a), the RFSI provides a reduction of HC emissions near $\phi = 0.6$ when the intake charge is not diluted. When the intake charge is diluted with nitrogen, hydrocarbon emissions increase due to the reduction in burn rate and the higher cycle-by-cycle combustion variation. For equivalence ratio values between 0.8 and 1.0, the HC increment is probably the consequence of a decreased HC burn-up due to lower expansion and exhaust stroke temperatures [40]. Further reduction of the equivalence ratio, $\phi < 0.8$, causes slow burning cycles, partial burning and even misfire occurring with increasing frequency, with a rapid increase of HC emissions. In these conditions, HC emissions are reduced with the RFSI due to its positive impact on combustion stability. At low engine loads, the positive effects of the RFSI on HC emissions are clearer, as shown in Fig. 18(b) at 4 bar imep.

Indicated specific NO*x* emissions are plotted in Fig. 19 versus the equivalence ratio. RFSI shows higher NO*x* emissions than the standard spark plug. In fact, combustion duration is shortened by the adoption of the RFSI, compared with the standard spark plug and, as a consequence, higher peak temperatures are attained, affecting NO*x* formation. At 8 bar imep, Fig. 19(a), NO*x* emission values without dilution are 1.5 g/kW h with the standard spark plug and 3.2 g/kW h with the RFSI at $\phi = 0.6$. A NO*x* emission value of 1.5 g/kW h is achieved with the RFSI at $\phi = 0.58$. Intake charge dilution considerably reduced NO*x* emissions for a given equivalence ratio. In this case, the minimum NO*x* emission value with the standard spark plug is 1.8 g/kW h at $\phi = 0.74$ and 2 g/kW h at $\phi = 0.67$ with the RFSI. NO*x* emissions reduce as the engine load reduces at constant speed, as shown in Fig. 19(b) at 4 bar imep.

6. Conclusion

A spark ignition internal combustion engine, equipped alternatively with a conventional spark plug and a radio frequency ignition system, was tested at different engine loads, equivalence ratio values and nitrogen dilution rates.

Initially, the RFSI electrode configuration was investigated, comparing the single and five electrodes RFSI. The 5 electrodes RFSI increased the heat losses, reducing the energy transfer efficiency

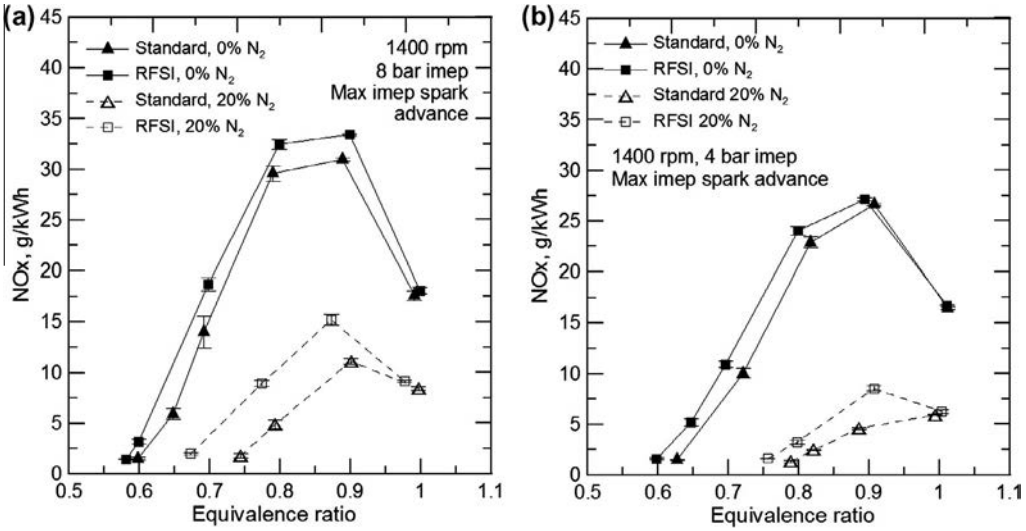

Fig. 19. Indicated specific NO*x* emissions versus the equivalence ratio with 0% and 20% intake air dilution with nitrogen.

from the spark to the gases, with lower performances compared to the single electrode RFSI at low equivalence ratio values and with dilution. The single electrode RFSI was finally chosen for the comparison with the standard spark plug.

The combustion duration was reduced by the adoption of the RFSI compared with the standard spark plug, with an increase of the engine efficiency ranging between 2% and 5% without dilution and between 1% and 4% with 20% nitrogen dilution. The RFSI extended the lean limit of combustion compared to the conventional spark plug at all test conditions and reduced the coefficient of variation of the indicated mean effective pressure, particularly at low equivalence ratio values and with nitrogen dilution.

RFSI provided a substantial benefit to CO and HC emissions, in particular when the intake charge was diluted. However, RFSI showed higher NO*x* emissions than the standard spark plug due to higher in-cylinder peak temperatures. It was possible to achieve the NO*x* emission values obtained with the standard spark plug also with the RFSI, exploiting its potential of extending the lean limit of combustion and the improved tolerance to dilution.

Results finally demonstrated that RFSI is an innovative ignition system that allows stable internal combustion engine operation with high dilution rates. RFSI also overcomes the compatibility problems of other non-conventional ignition systems.

References

[1] Wei H, Zhu T, Shu G, Tan L, Wang Y. Gasoline engine exhaust gas recirculation – a review. Appl Energy 2012;99:534–44.

[2] Gallon E, Fontana G, Palmaccio R. Effects of exhaust gas recycle in a downsized gasoline engine. Appl Energy 2013;105:99–107.

[3] Galloni E, Fontana G, Palmaccio R. Numerical analyses of EGR techniques in a turbocharged spark-ignition engine. Appl Thermal Eng 2012;39:95–104.

[4] Kuroda H, Nakajima Y, Sugihara K, Takagi Y et al. The fast burn with heavy EGR, new approach for low NO*x* and improved fuel economy. SAE technical paper; 1978 [780006].

[5] Quader A. What limits lean operation in spark ignition engines-flame initiation or propagation. SAE technical paper; 1976 [760760].

[6] Fontana G, Galloni E. Experimental analysis of a spark-ignition engine using exhaust gas recycle at WOT operation. Appl Energy 2010;87:2187–93.

[7] Stuhlman Jr O. The extension of Paschen's law to include the electrodeless glow discharge. J Franklin Inst 1932;213(3):273–82.

[8] Tardiveau P, Marode E, Agneray A, Cheaib M. Pressure effects on the development of an electric discharge in non-uniform fields. J Phys D: Appl Phys 2001;34:1690–6.

[9] Van Veldhuizen EM, Briels TMP, Ebert U. Branching of positive discharge streamers in air at varying pressures. IEEE Trans Plasma Sci 2005;33(2):264–5.

[10] Dale JD, Checkel MD, Smy PR. Application of high energy ignition systems to engines. Prog Energy Combust Sci 1997;23(5–6):379–98.

[11] Hood S. The V-grooved electrode spark plug. SAE technical paper; 1990 [901535].

[12] Lenk M, Podiak R. Copper cored ground electrode spark plug design. SAE technical paper; 1988 [881777].

[13] Nakamura N, Baika T, Shibata Y. Multipoint spark ignition for lean combustion. SAE technical paper; 1985 [852092].

[14] Gettel LE, Tsai KC. Flame kernel development with the multiple electrode spark plug. Combust Flame 1983;54(1–3):225–8.

[15] Latsch R. The swirl-chamber spark plug: a means of faster, more uniform energy conversion in the spark-ignition engine. SAE technical paper; 1984 [840455].

[16] Morsy MH. Review and recent developments of laser ignition for internal combustion engines applications. Renew Sustain Energy Rev 2012;16:4849–75.

[17] Phuoc TX, White FP. Laser-induced spark ignition of CH_4/air mixtures. Combust Flame 1999;119:203–16.

[18] Asik J, Piatkowski P, Foucher M, Rado W. Design of a plasma jet ignition system for automotive application. SAE technical paper; 1977 [770355].

[19] Dale J, Oppenheim A. Enhanced ignition for i.c. engines with premixed gases. SAE technical paper; 1981 [810146].

[20] Edwards C, Oppenheim A, Dale J. A comparative study of plasma ignition systems. SAE technical paper; 1983 [830479].

[21] Kupe J, Wilhelmi H, Adams W. Operational characteristics of a lean burn sl-engine: comparison between plasma-jet and conventional ignition system. SAE technical paper; 1987 [870608].

[22] Karim G, Al-Himyary T, Dale J. An examination of the combustion processes of a methane fuelled engine when employing plasma jet ignition. SAE technical paper; 1989 [891639].

[23] Hall M, Tajima H, Matthews R, Koeroghlian M et al. Initial studies of a new type of ignitor: the railplug. SAE technical paper; 1991 [912319].

[24] Matthews R, Hall M, Faidley R, Chiu J et al. Further analysis of railplugs as a new type of ignitor. SAE technical paper; 1992 [922167].

[25] Heise V, Farah P, Husted H, Wolf E. High frequency ignition system for gasoline direct injection engines. SAE technical paper; 2011 [2011-01-1223].

[26] Ikeda Y, Nishiyama A, Wachi Y, Kaneko M. Research and development of microwave plasma combustion engine (Part I: concept of plasma combustion and plasma generation technique). SAE technical paper; 2009 [2009-01-1050].

[27] Ikeda Y, Nishiyama A, Katano A, Kaneko M, Jeong H. Research and development of microwave plasma combustion engine (Part II: engine performance of plasma combustion engine). SAE technical paper; 2009 [2009-01-1049].

[28] Nishiyama A, Ikeda Y. Improvement of lean limit and fuel consumption using microwave plasma ignition technology. SAE technical paper; 2012 [2012-01-1139].

[29] Wolk B, DeFilippo A, Chen J, Dibble R, Nishiyama A, Ikeda Y. Enhancement of flame development by microwave-assisted spark ignition in constant volume combustion chamber. Combust Flame 2013;160(7):1225–34.

[30] Sher E, Ben-Ya'ish J, Pokryvailo A, Spector Y. A corona spark plug system for spark-ignition engines. SAE technical paper; 1992 [920810].

[31] Liu JB, Ronney PD, Gundersen MA. Premixed flame ignition by transient plasma discharges. In: the twenty-ninth international symposium on combustion, Sapporo; 2002.

[32] Starikovskaia SM. Plasma assisted ignition and combustion. J Phys D: Appl Phys 2006;39:R265–99.

[33] Starikovskiy A, Aleksandrov N. Plasma-assisted ignition and combustion. Prog Energy Combust Sci 2013;39(1):61–110.

[34] Shiraishi T, Kakuho A, Urushihara T, Cathey C, et al. A study of volumetric ignition using high-speed plasma for improving lean combustion performance in internal combustion engines. SAE Int J Eng 2009;1(1):399–408.
[35] Agneray A, Jaffrezic X, Pariente M, Makarov M, Nouvel C, Deloraine F, Mispreuve L, Roque F, Dumont T. Radio frequency ignition system. Breakthrough technology for the future spark ignition engine. SIA; 2006.
[36] Stiles R, Thompson G, Smith J. Investigation of a radio frequency plasma ignitor for possible internal combustion engine use. SAE technical paper; 1997 [970071].
[37] Tardiveau P. Contribution à l'étude du déclenchement de la combustion par décharge électrique en milieu diphasique. PhD thesis; 2002 [Université Paris 6].
[38] Auzas F. Décharge radiofréquence produite dans les gaz à pression élevée pour le déclenchement de combustion. PhD thesis; 2008 [Université Paris Sud–XI].
[39] Woschni G. A universally applicable equation for the instantaneous heat transfer coefficient in the internal combustion engine. SAE technical paper; 1967 [670931].
[40] Heywood JB. Internal combustion engines fundamentals. New York: Mc Graw-Hill; 1989.
[41] Klimstra J. The optimum combustion phasing angle—a convenient engine tuning criterion. SAE technical paper; 1985 [852090].